LLNL-PRES-676629

Closure Models for High-Order Finite Element Hydrodynamics

MultiMat 2015, Würzburg, Germany

September 8, 2015

R. Anderson, T. Brunner, V. Dobrev, Tz. Kolev, R. Rieben and V. Tomov

Lawrence Livermore National Laboratory

This work was performed under the auspices of the U.S. Department of Energy by Lawrence Livermore National Laboratory under Contract DE-AC52-07NA27344. Lawrence Livermore National Security, LLC

We develop novel high-order multi-physics numerical methods for future hardware

- We use the Arbitrary Lagrangian-Eulerian (ALE) framework to simulate the equations of shock hydrodynamics.
- High-order Finite Element Methods could provide better simulation quality.
- High-order Finite Element Methods promise better efficiency on Future Systems.
- Increasing the order produces more flops with the same data motion.

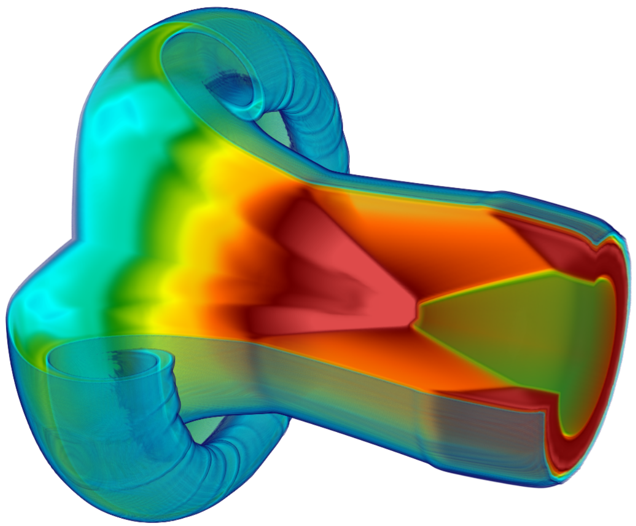

3D ALE simulation of a shock interaction

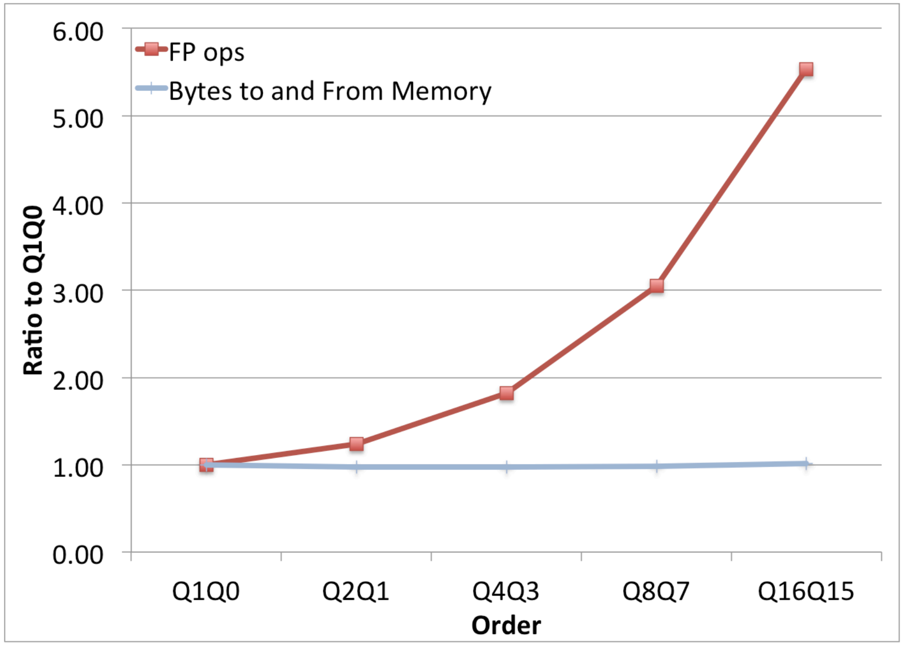

Example – shock passing through an equilibrated cell

Pure cells

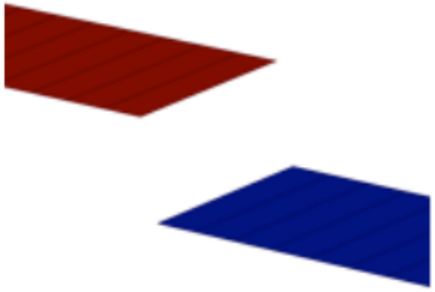

Mixed cell

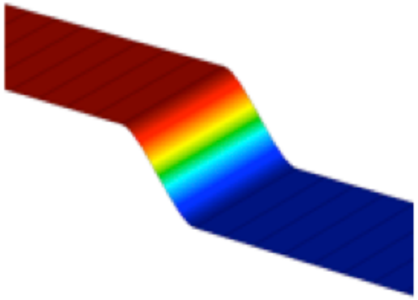

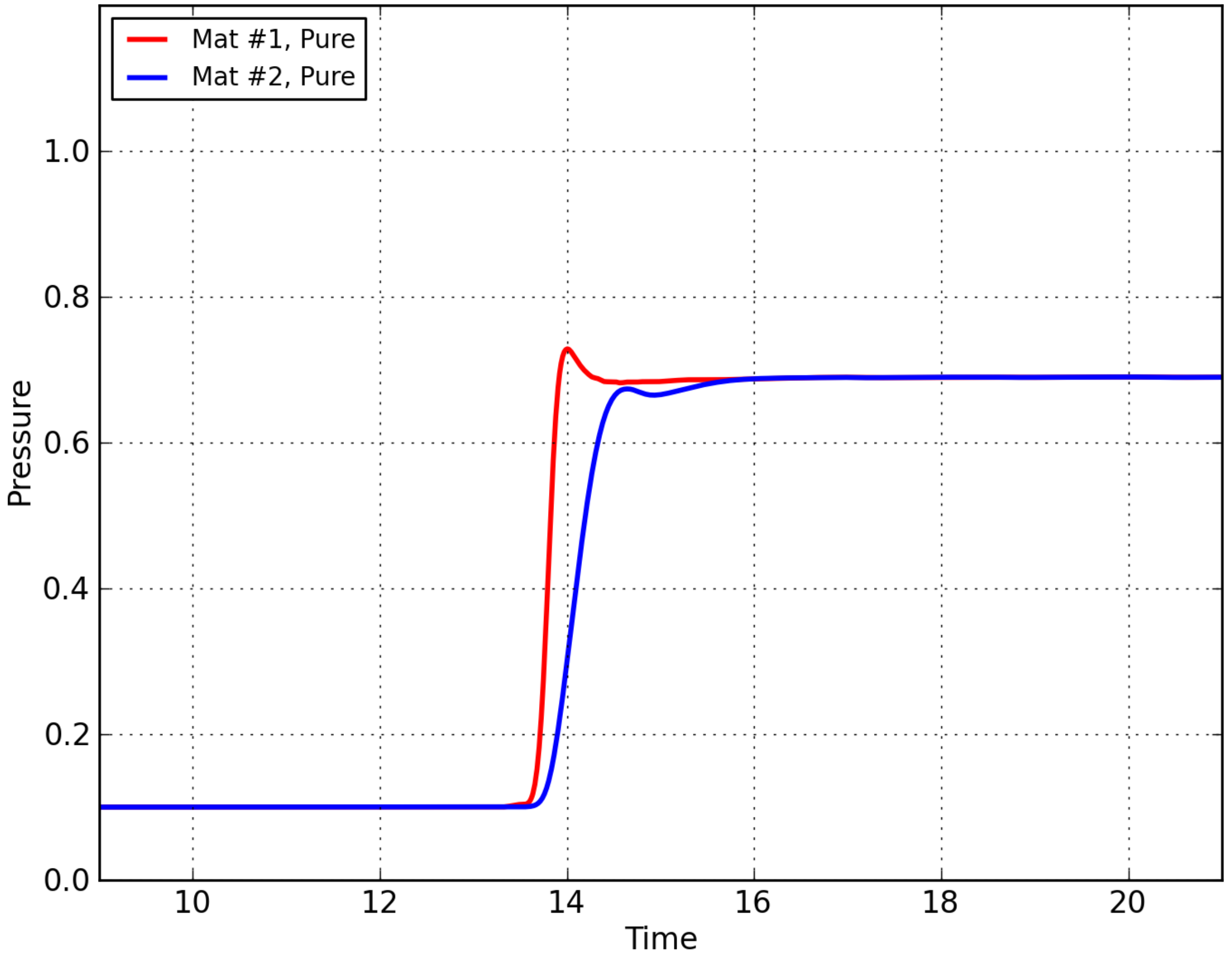

Example – shock passing through an equilibrated cell

Pure cells

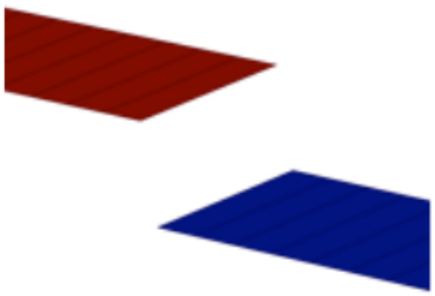

Mixed cell

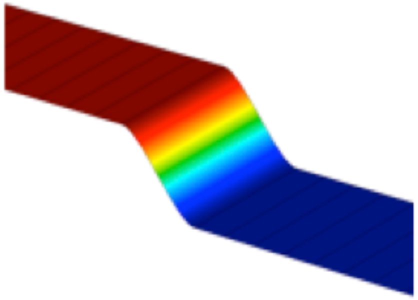

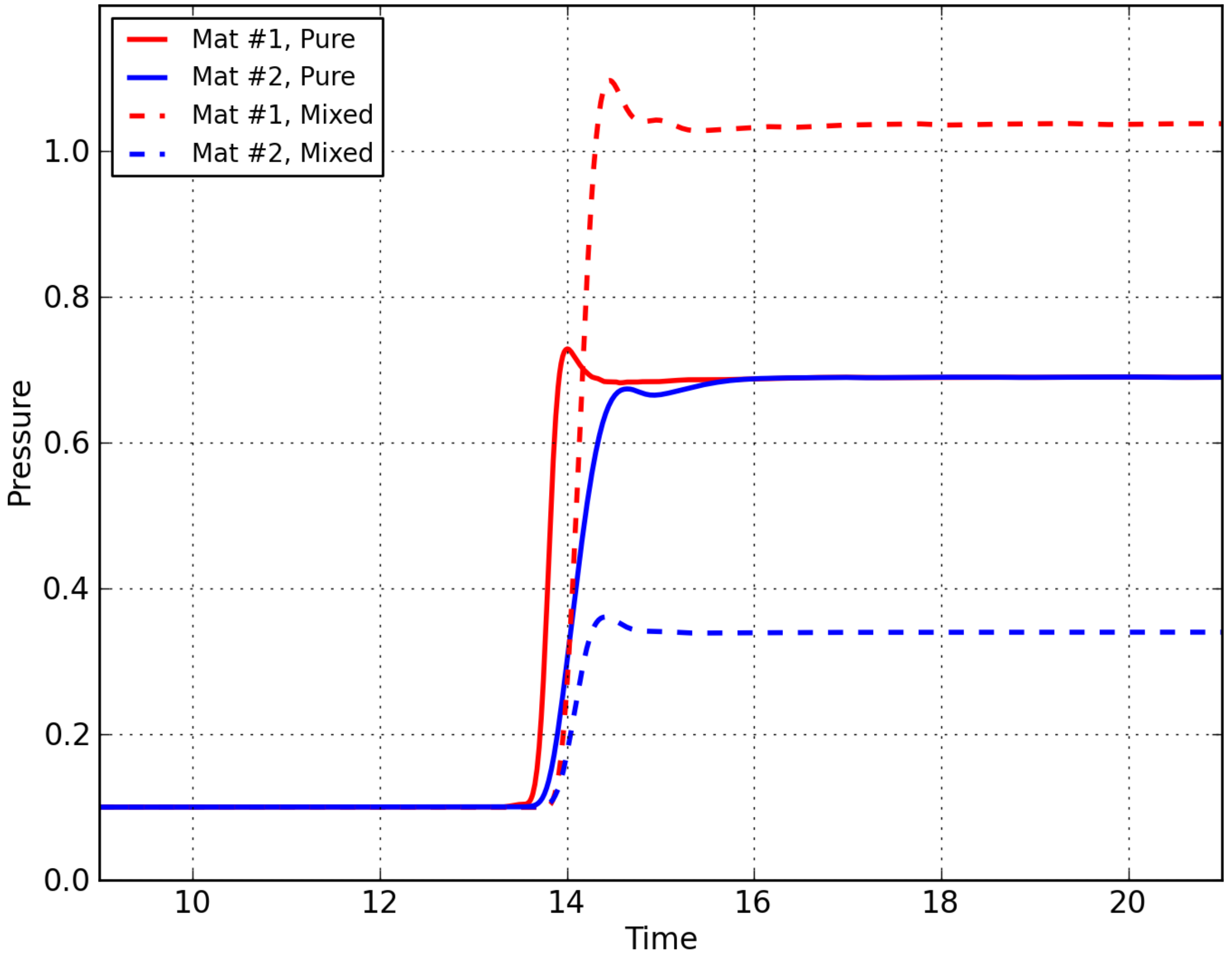

Example – shock passing through an equilibrated cell

Pure cells

Mixed cell

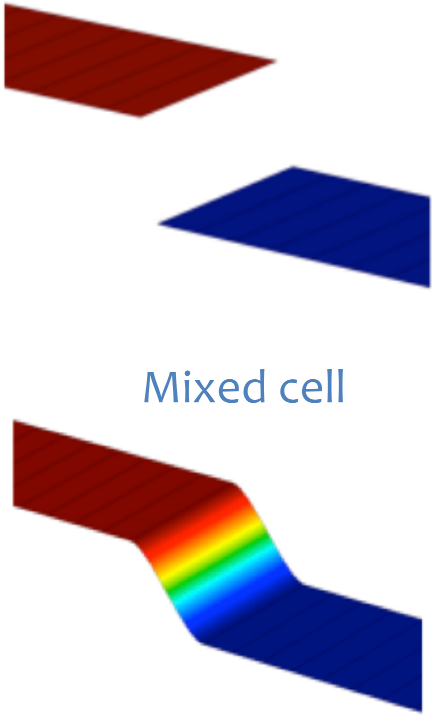

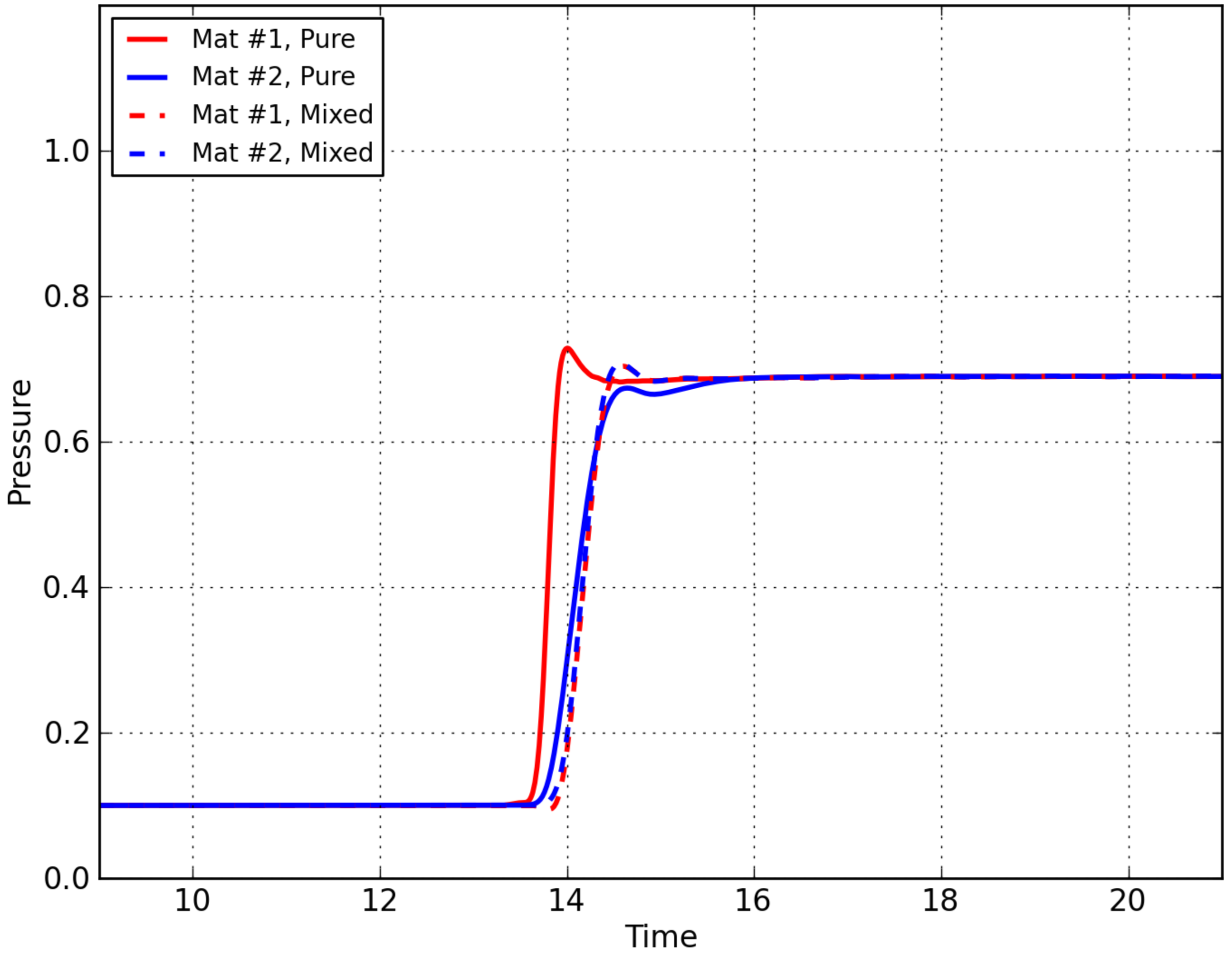

References

- R. Tipton, *“CALE mixed zone pressure relaxation model,”* unpublished notes, 1989
- D. Miller, G. Zimmerman, *“An algorithm for time evolving volume fractions in mixed zones in Lagrangian hydrodynamics calculations,”* 2009
- A. Barlow, *“A new Lagrangian scheme for multimaterial cells,”* 2001
- A. Barlow, R. Hill, M. Shashkov, *"Constrained optimization framework for interface-aware sub-scale dynamics closure model for multimaterial cells in Lagrangian and arbitrary Lagrangian–Eulerian hydrodynamics,”* 2014
- J. Kamm, M. Shashkov, J. Fung, A. Harrison, T. Canfield, *"A comparative study of various pressure relaxation closure models for one-dimensional two-material Lagrangian hydrodynamics,”* 2010
- Yu. Yanilkin, E. Goncharov, V. Kolobyanin, V. Sadchikov, J. Kamm, M. Shashkov, W. Rider, *“Multi-material pressure relaxation methods for Lagrangian hydrodynamics,”* 2013

We derive a closure model that is compatible with our high-order finite element framework

- Pressure relaxation on integration point level
- Sub-cell computations with no material interfaces
- General with respect to high-order discretizations in space and time

3 – material cell tracking 121 points, Q6Q5, RK4

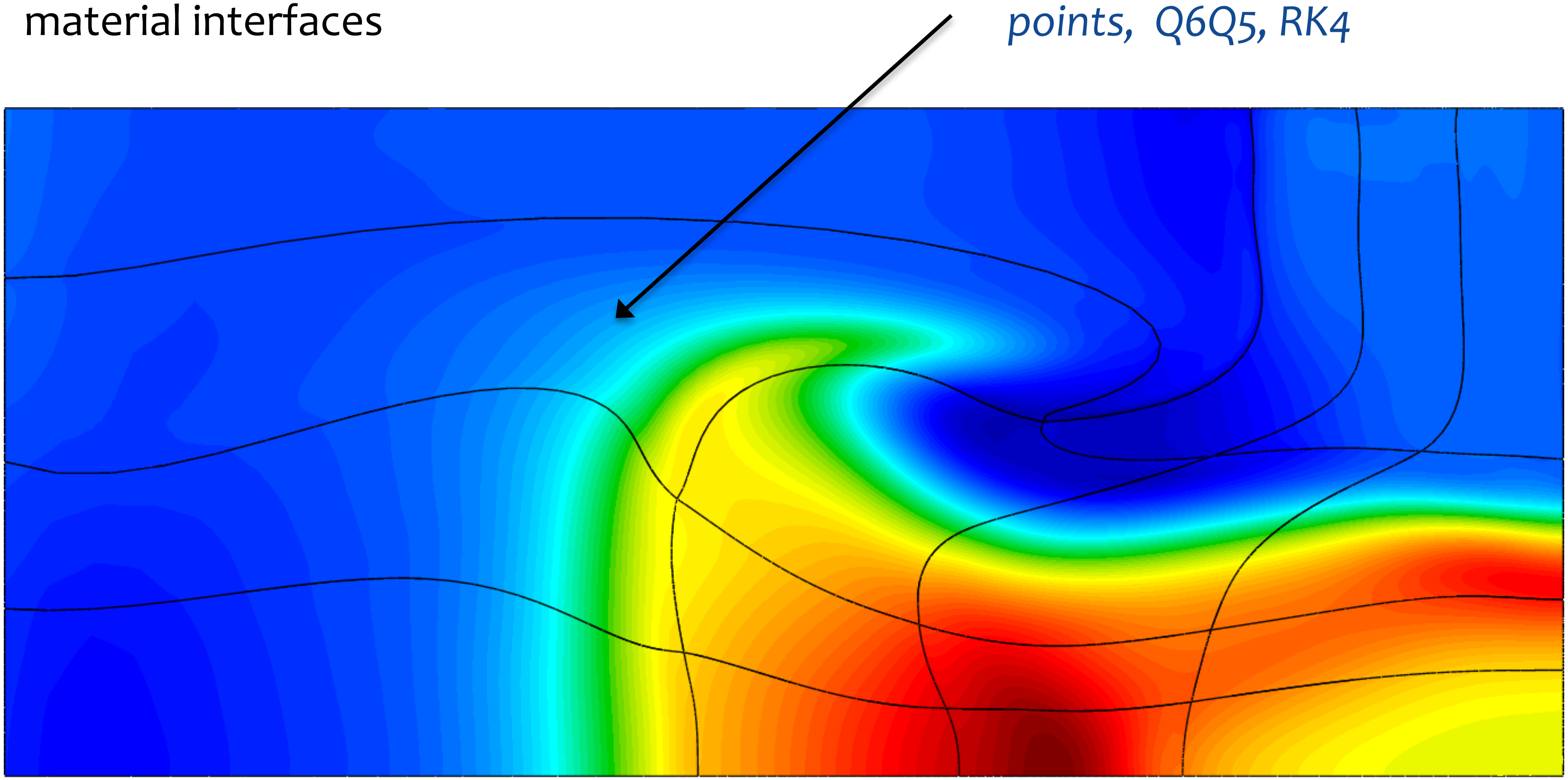

We define our material representation on continuous level

- We evolve a single velocity and multiple, material-specific thermodynamic variables.

- Material indicator functions:

$$V_k = \int \eta_k \rightarrow \eta_k(x) = \frac{V_k(x)}{V(x)}$$

$$\sum_k \eta_k = 1\,, \quad 0 \le \eta_k \le 1$$

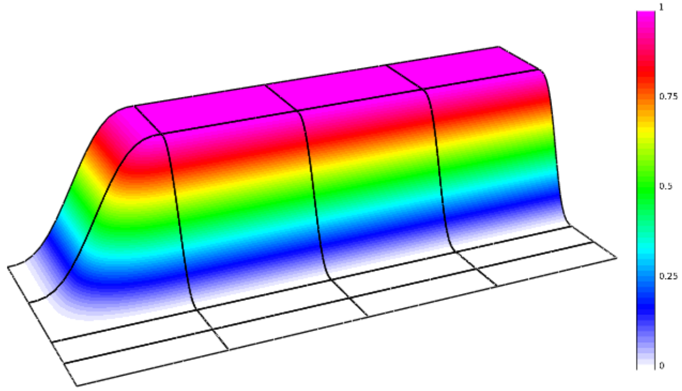

Initial indicator function

- Density and specific internal energy:

$$M_k = \int \eta_k \rho_k\,,\, I_k = \int \eta_k \rho_k e_k$$

$$\rho = \sum_k \eta_k \rho_k\,, \quad \rho e = \sum_k \eta_k \rho_k e_k$$

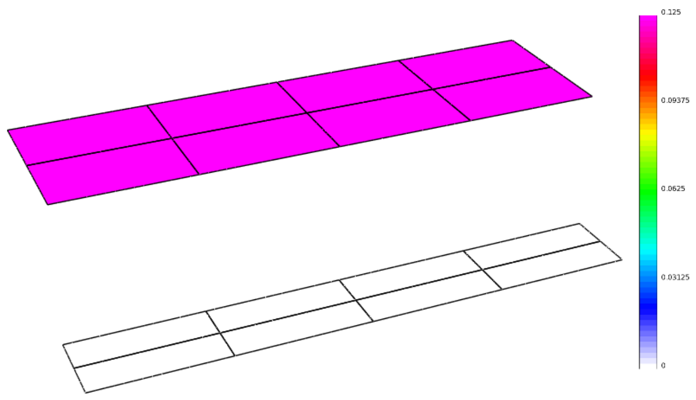

Initial density extension

Multi-material evolution is defined through a continuous model

- Differences in compressibility are recognized by $\beta_k = \frac{dV_k}{dV}\,, \sum_k \beta_k = 1$

- Evolution of indicators and material mass conservation:

$$\frac{d\eta_k}{dt} = (\beta_k - \eta_k)\nabla \cdot v\,, \qquad \frac{d(\eta_k \rho_k)}{dt} = -\eta_k \rho_k \nabla \cdot v.$$

- Momentum and specific internal energy:

$$\eta_k \rho_k \frac{de_k}{dt} = -\beta_k p_k \nabla \cdot v$$

$$\rho \frac{dv}{dt} = -\nabla \sum_k \beta_k p_k$$

Non-convex combination

$\longrightarrow$

$$\eta_k \rho_k \frac{de_k}{dt} = -\eta_k p_k \nabla \cdot v - c_p(\beta_k - \eta_k) p^* \nabla \cdot v$$

$$\rho \frac{dv}{dt} = -\nabla \sum_k \eta_k p_k$$

Our high-order closure models are based on point-wise pressure equilibration

$$dp = -\kappa \frac{dV}{V}$$

Material Bulk Modulus

- Fully-discrete pressure prediction at each point

$$p_k' = p_k^n - \tau \kappa_k \frac{\beta_k}{\eta_k} \nabla \cdot v = \bar{p}_k - \tau \kappa_k \frac{(\beta_k - \eta_k)}{\eta_k} \nabla \cdot v$$

- Pressure equilibration imposed by $p_k' = p^*$

$$p^* = \sum_k \left(\bar{p}_k \frac{\eta_k}{\kappa_k} \right) / \left(\sum_k \frac{\eta_k}{\kappa_k} \right)$$

$$(\beta_k - \eta_k) \nabla \cdot v = \frac{1}{\tau} (\bar{p}_k - p^*) \frac{\eta_k}{\kappa_k}$$

Equilibration time scale at the point of interest

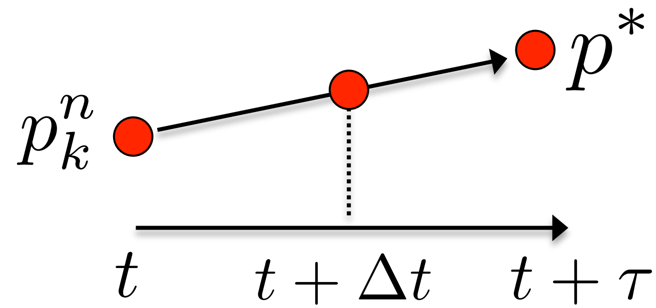

$$\tau = c_\tau \min_k \left(\frac{h}{C_{s,k}} \right)$$

Additional discretization details

- Material indicators are not FE functions
  - Evolved at quadrature points, not DOFs

$$\eta_k^* = \eta_k + c\Delta t(\beta_k - \eta_k)\nabla \cdot v$$

- Limiting is applied at each integration point

$$|c\Delta t(\beta_k - \eta_k)\nabla \cdot v| \leq 0.5\eta_k \,, \quad \sum_k \eta_k^* = 1 \,, \quad 0 < \eta_k^* < 1$$

- The energy equations use the limited quantities and a common pressure

$$\eta_k \rho_k \frac{de_k}{dt} = -\eta_k p_k \nabla \cdot v - c_p p^* (\beta_k - \eta_k)\nabla \cdot v + \eta_k \sigma_{a,k} : \nabla v$$

  - Minimizing the error leads to $c_p = \dfrac{\sum_k p_k (\beta_k - \eta_k)^2}{\sum_k p^* (\beta_k - \eta_k)^2}$ ✗

- Each material computes its own viscosity. $\sigma_a = \sum_k \eta_k \sigma_{a,k}$

Modified Sod shock tube

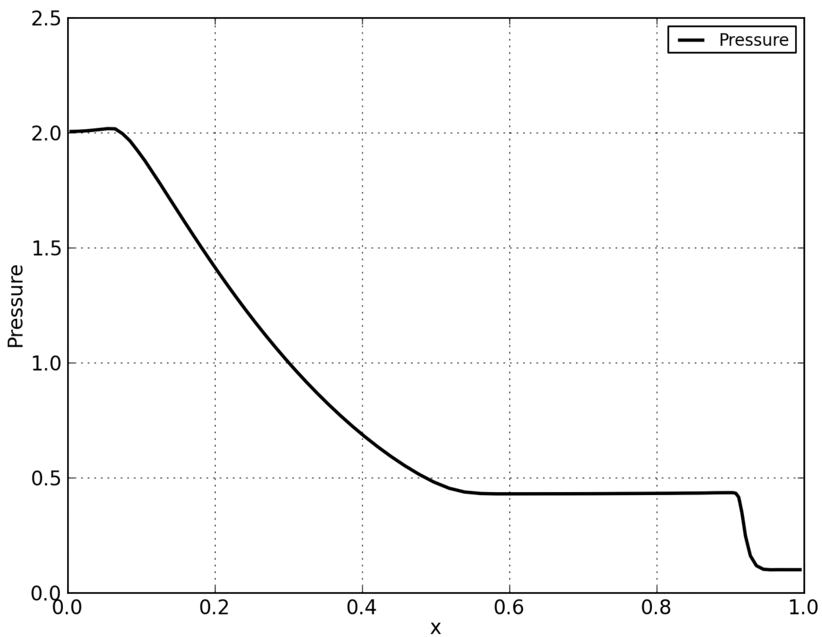

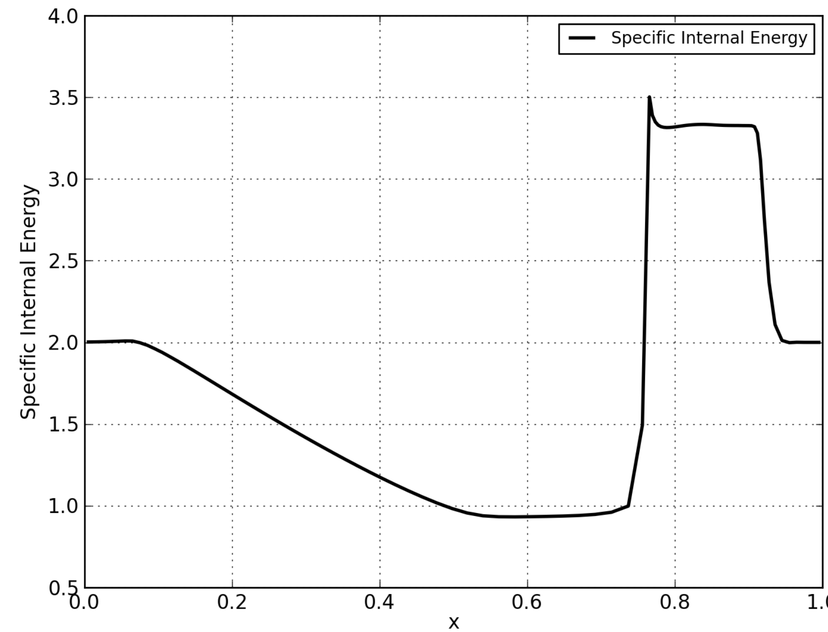

Modified Sod shock tube – 1st order

Q1Q0, 1 point
RK2, 100 cells

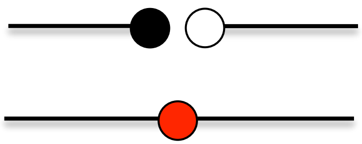

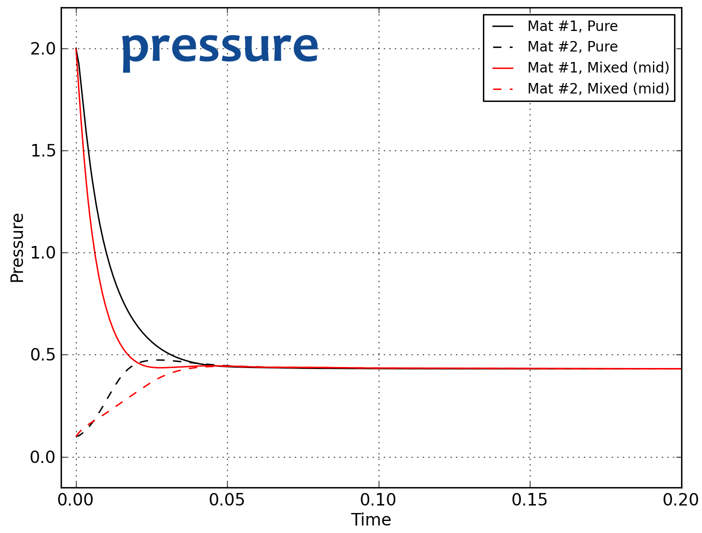

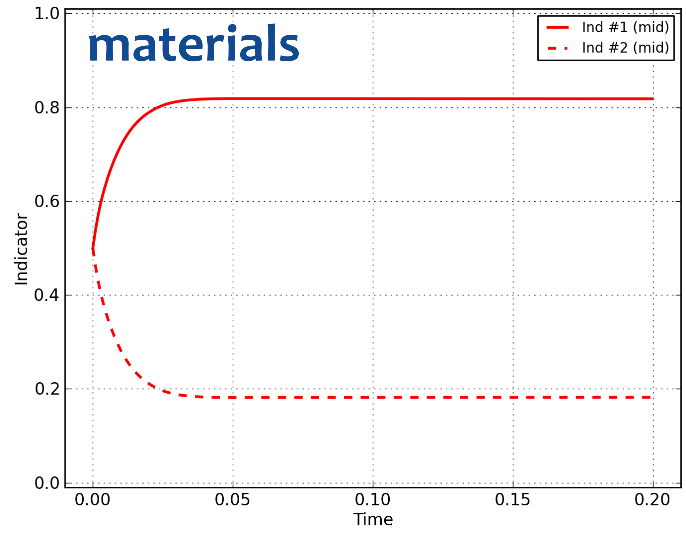

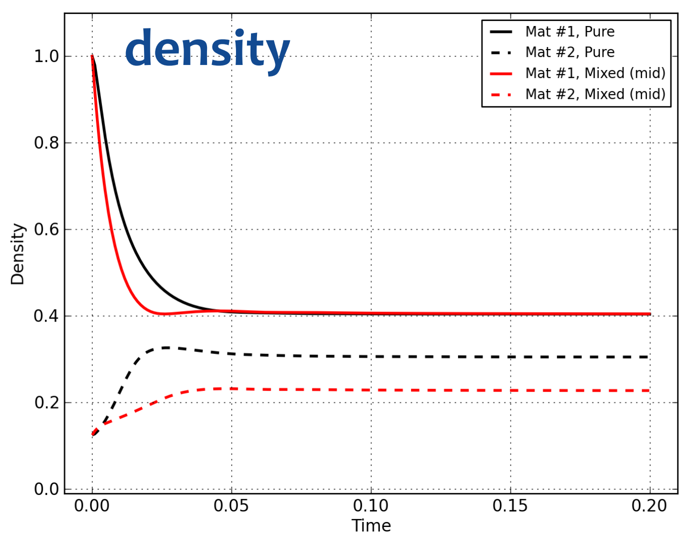

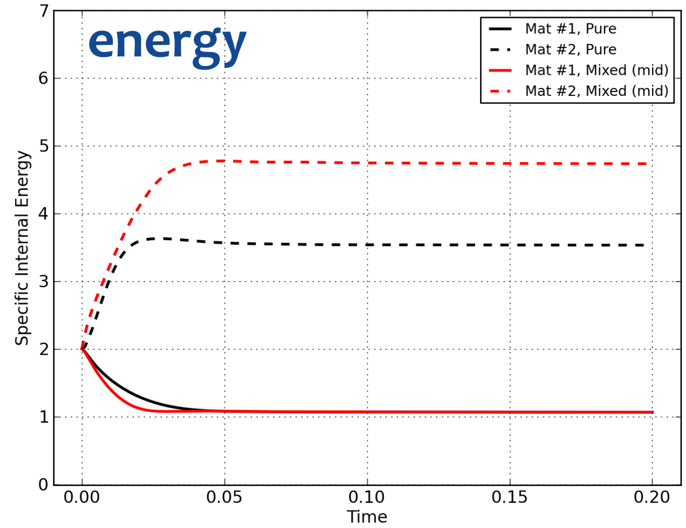

Modified Sod shock tube – 3^{rd} order

Q3Q2, 5 points
RK4, 20 cells

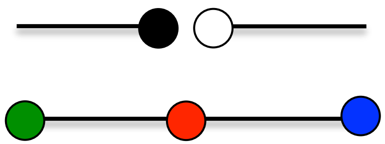

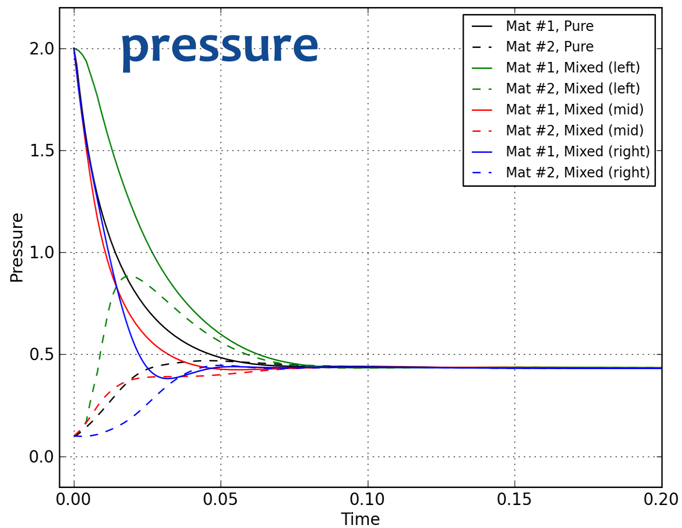

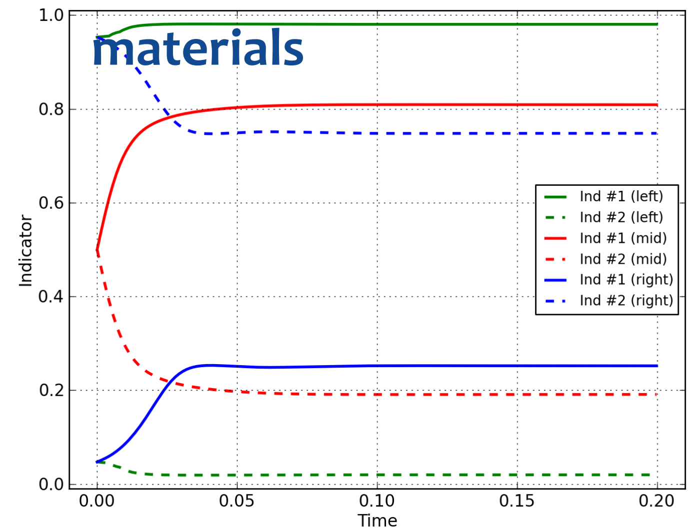

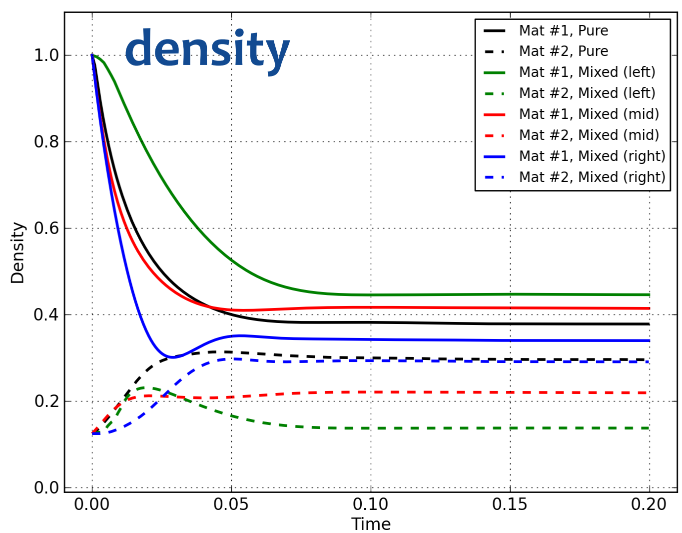

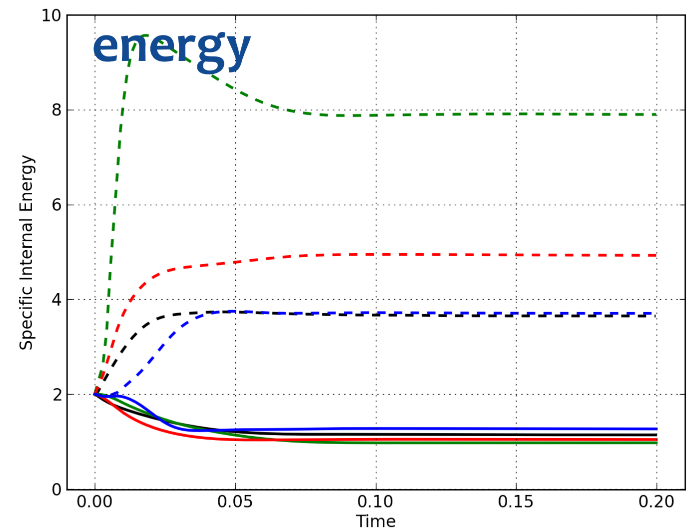

Water / air shock tube

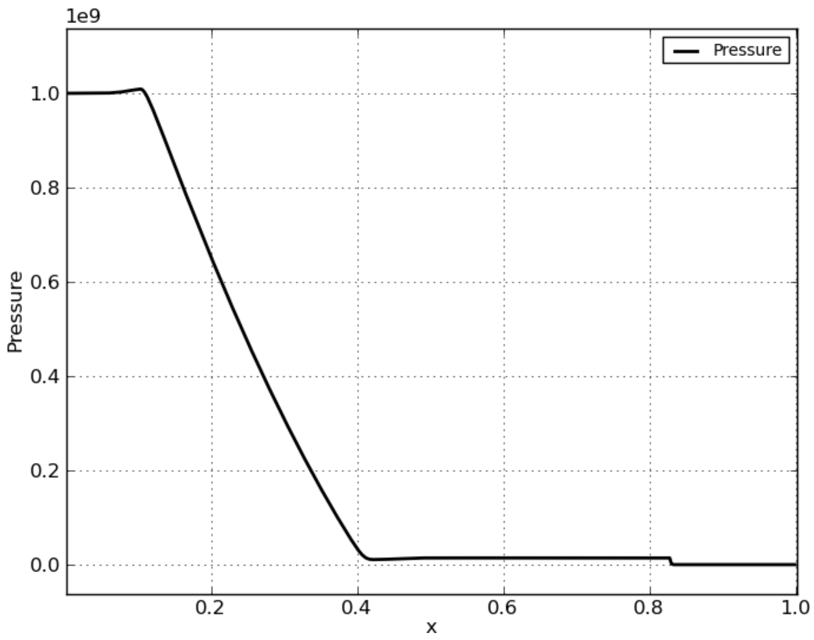

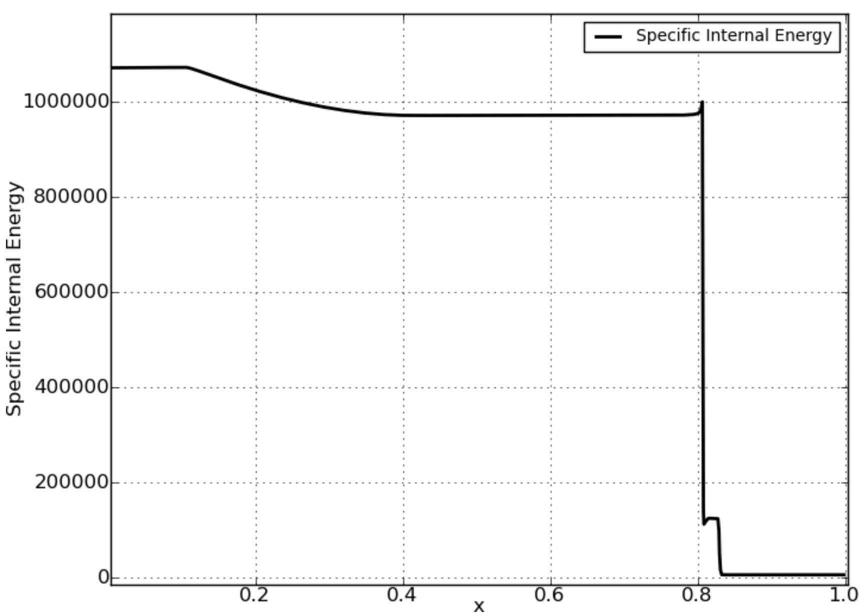

Water / air shock tube – 1st order

Q1Q0, 1 point
RK2, 500 cells

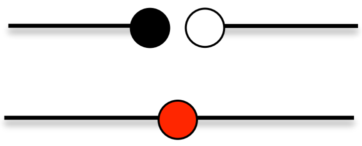

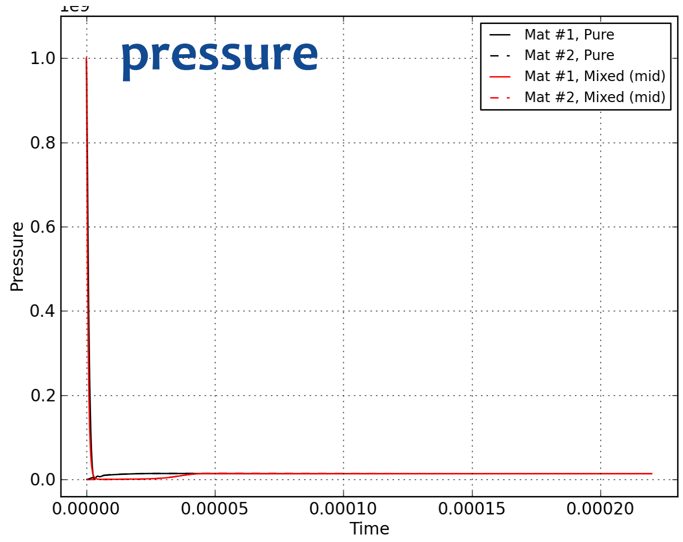

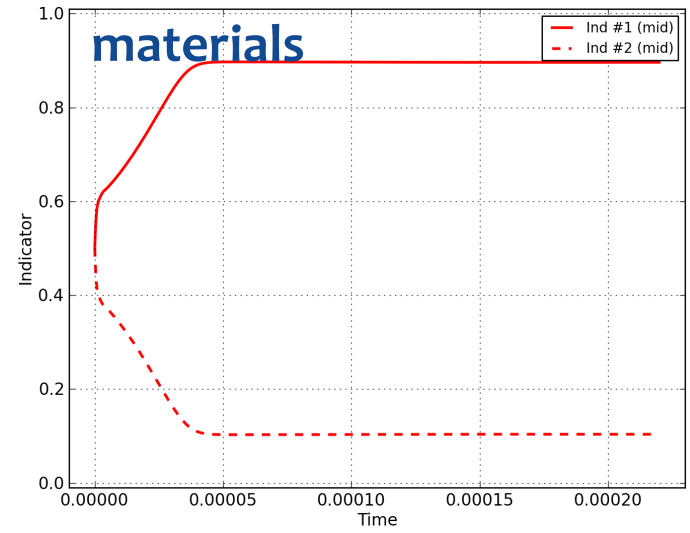

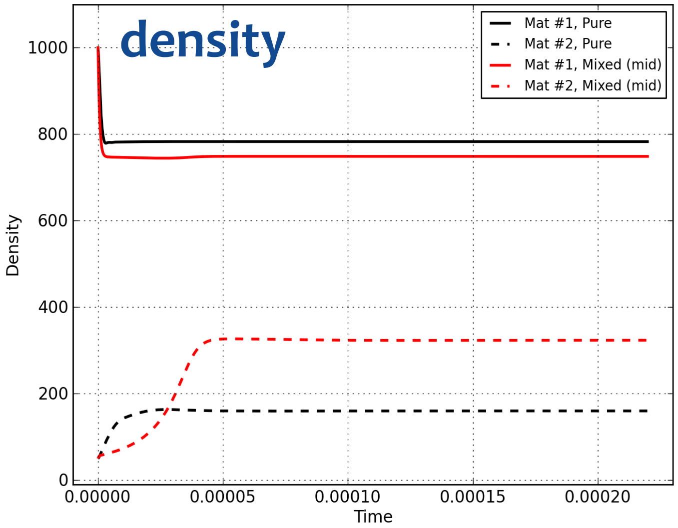

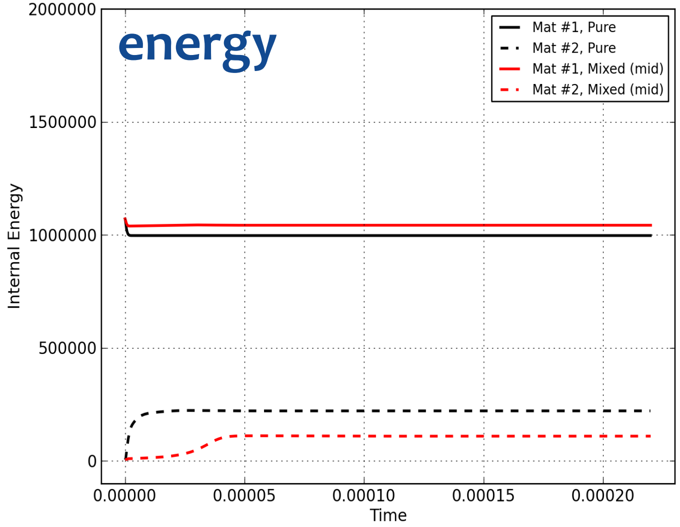

Water / air shock tube – 3rd order

Q3Q2, 5 points
RK4, 100 cells

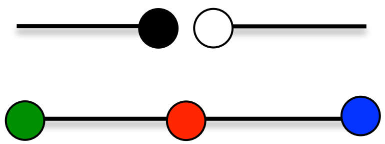

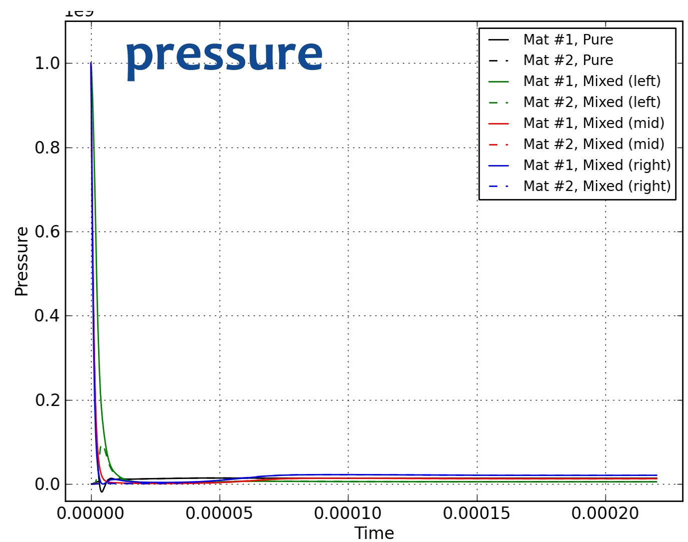

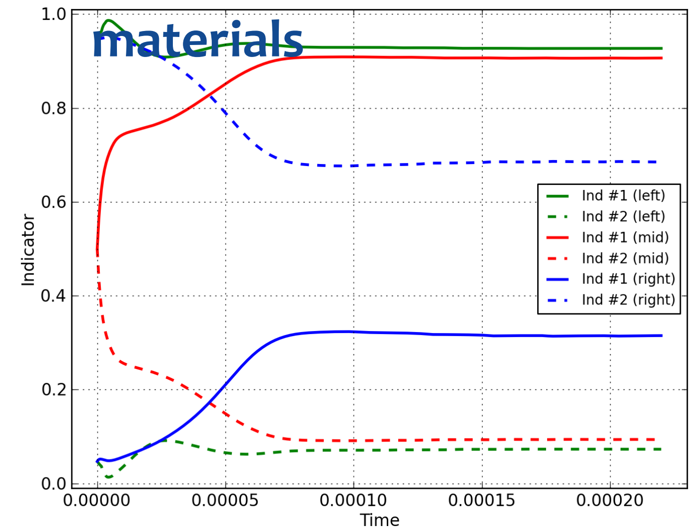

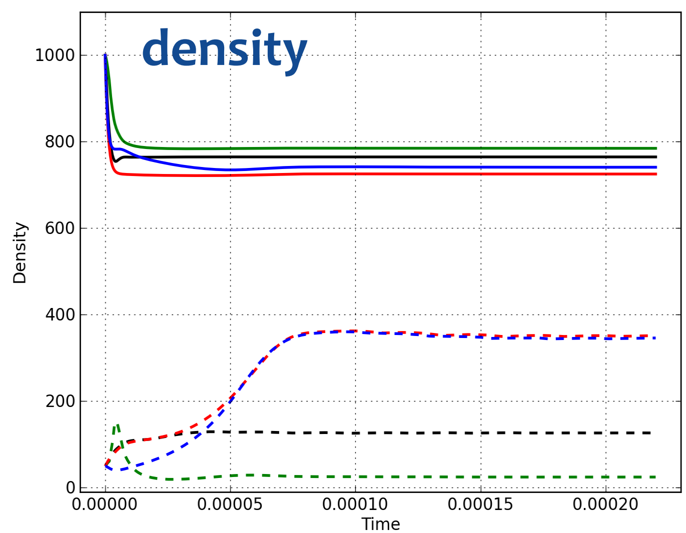

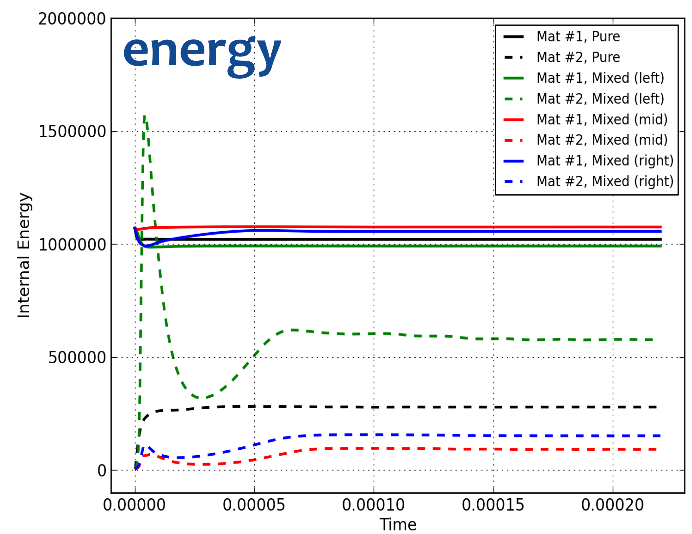

Steel ball impacting an Aluminum plate – 2nd order

Axisymmetric

Air + Steel + Al

Gruneisen, no strength

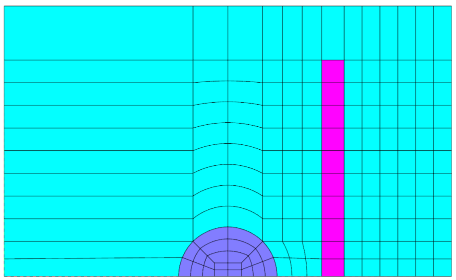

Q2Q1 + RK2

NURBS coarse mesh (generated by PMESH)

High-order ALE + High-order Closure

The closure model is necessary to avoid sensitivity to the EOS

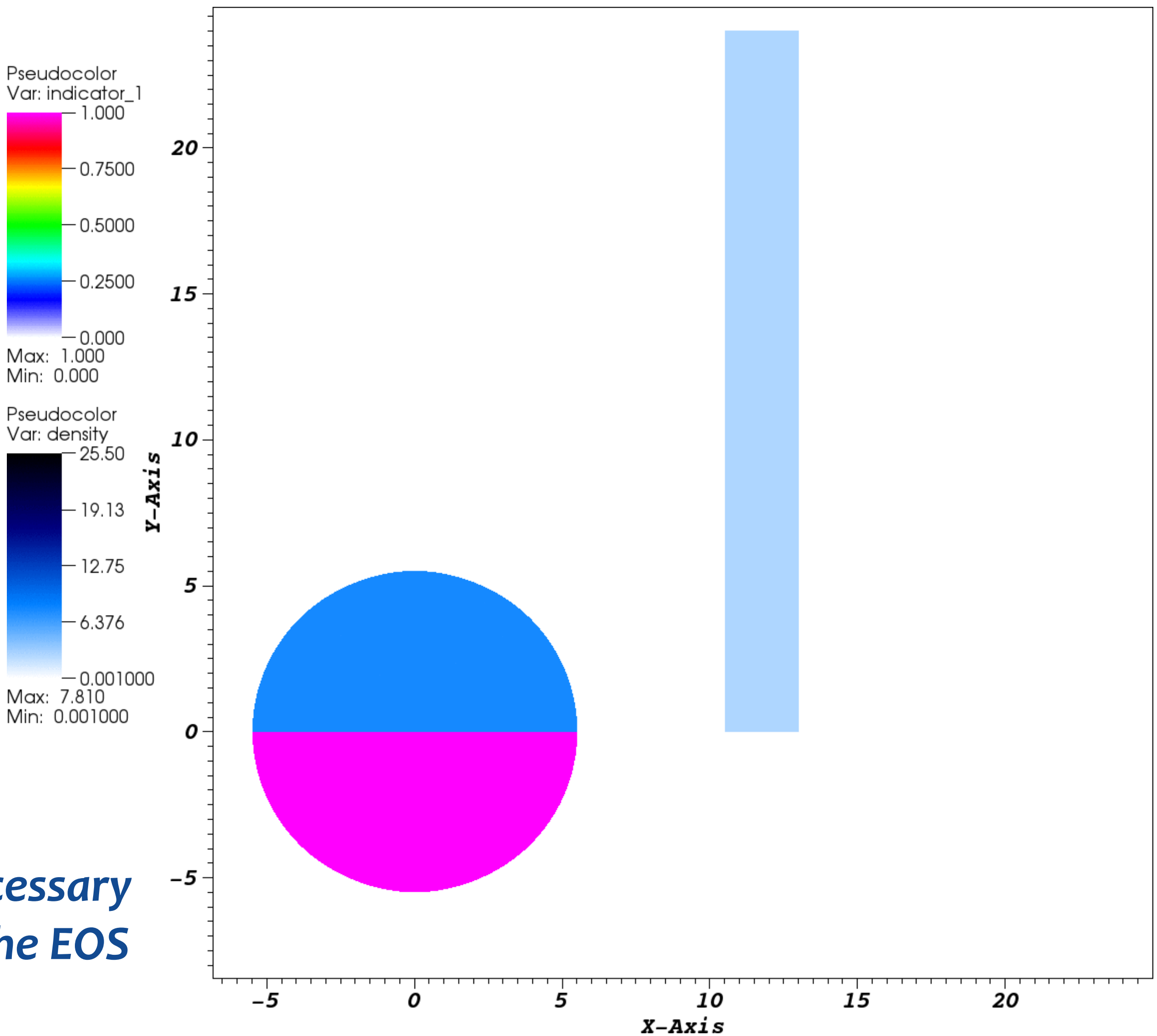

Steel ball impacting an Aluminum plate – 2nd order

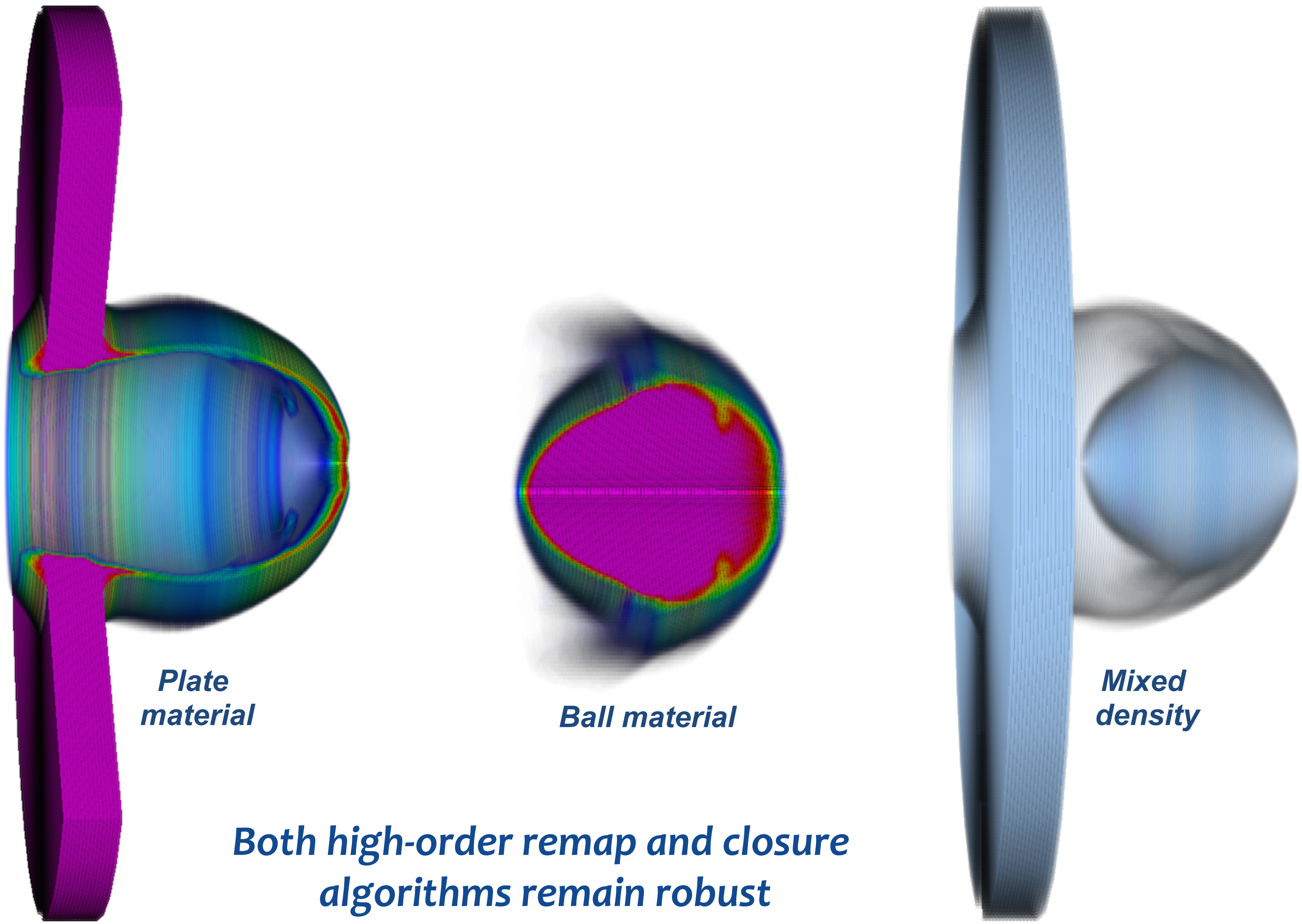

Both high-order remap and closure algorithms remain robust

Conclusions and future work

- High-order closure models show promise:
  - Applicable to high-order elements on curved meshes
  - Applicable to high-order time integrators
  - Sub-cell resolution without reconstruction of explicit material interfaces (currently)
- We continue the closure research:
  - Improvements for small amounts of material that is being compressed
  - Better calculation of energy redistribution
- Other high-order research topics:
  - Performance improvements on modern architectures
  - High-order radiation diffusion coupled with ALE hydro
  - High-order non-conforming AMR

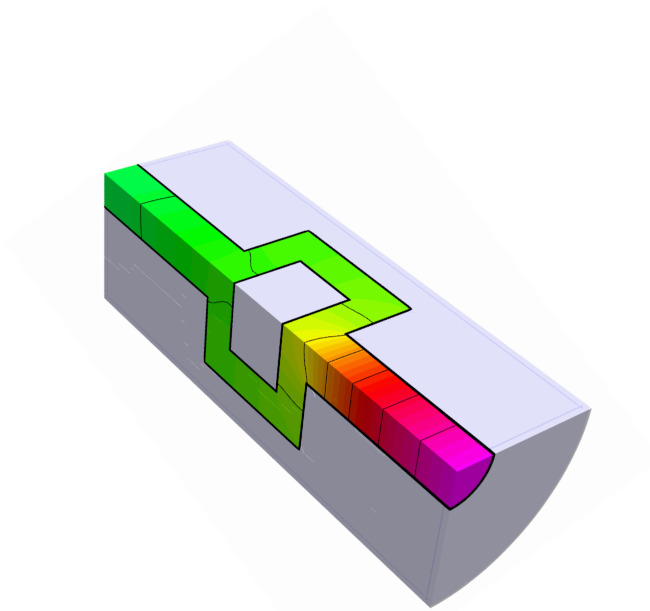

Crooked pipe, Q2-Q1

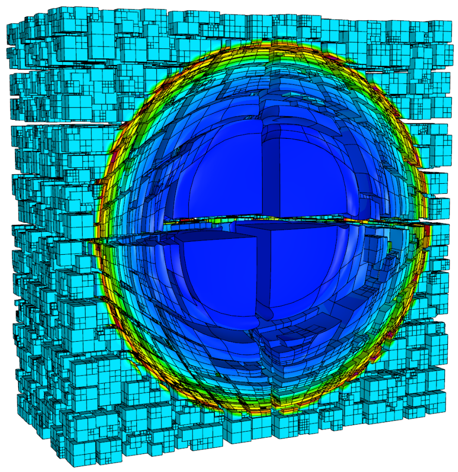

Sedov, parallel NMR